# Effect of Cu and Mg contents on similar and dissimilar welding of 7XXX series aluminum alloys

M. El-Shennawy [a], A.A. Omar [b] and M.I. Masoud [a]
[a] *Industrial Eng. Dept., Faculty of Eng., Cairo University-Fayoum Branch, El-Fayoum 63111, Egypt*
*e-mail: moha_111@yahoo.com and ibrahim_64@yahoo.com*
[b] *Mechanical Eng. Dept., Benha High Institute of Technology, Benha, Egypt*
*e-mail: adelomar2004@yahoo.com*

This research discusses the various effects of alloying elements specially Cu and Mg contents on the weldability of Al-Zn-Mg-Cu-based alloy (7*xxx* series). Five series having different chemical compositions have been adopted. Both similar and dissimilar fusion welded joints have been made through various combinations of such alloys. Examination of mechanical properties of the welded joints; tensile strength and hardness values were carried out coupled with microstructure examination for the alloys before and after welding. This research could explain the effects of alloying additions; Cu and Mg, on the weldability of Al-Zn-Mg-Cu- based alloys. Increasing Cu content to about 2.83 wt% with almost zero Mg showed the best tensile strength either in similar or dissimilar welded joints. Same results could be obtained with maximum content of Mg: 2.42 wt% and almost zero Cu. Increasing both Cu and Mg contents to 2.42 wt% and 2.53 wt%, respectively in the same time deteriorated the tensile strength for similar and dissimilar welded joints. Welding of Al-Zn-Mg-Cu alloy has an inverse relation with combined increase of Cu and Mg content while it has a direct relation with single increase of either Cu or Mg alloying addition.

هذا البحث يناقش التأثيرات المختلفة لعنصرى النحاس والماغنيسيوم على قابلية لحام سبيكة الألومنيوم Al-Zn-Mg-Cu من عائلة 7*xxx*. تم عمل خمس مجموعات من هذه السبيكة ذات تركيب كيميائى مختلف مع إعداد عينات لحام متماثل وغير متماثل من هذه السبيكة بطريقة لحام الانصهار. أجريت الاختبارات الميكانيكية: الشد والصلادة، بالإضافة إلى دراسة البنية المجهرية للمجموعات المختلفة قبل وبعد اللحام. أشارت نتائج هذا البحث إلى أن السبيكة ذات أعلى نسبة نحاس مستخدمة في هذا البحث وهى ٢,٨٣% ونسبة ماغنيسيوم حوالى صفر % سجلت أعلى قيمة إجهاد شد في كلتا حالتى اللحام المتماثل وغير المتماثل. وبالمثل فإن السبيكة ذات أعلى نسبة ماغنيسيوم مستخدمة في هذا البحث وهى ٢,٤٢% ونسبة نحاس حوالى صفر % سجلت أعلى قيمة إجهاد شد في كلتا حالتى اللحام المتماثل وغير المتماثل. على الجانب الآخر، فإن زيادة كل من النحاس والماغنيسيوم إلى ٢,٨٣% و ٢,٤٢% على الترتيب في نفس الوقت أدى إلى تدهور متانة الوصلات المتماثلة وغير المتماثلة حيث سجلت أقل قيم إجهاد شد. وعليه يخلص البحث إلى أن قابلية لحام سبيكة Al-Zn-Mg-Cu تتناسب عكسيا مع زيادة كل من النحاس والماغنيسيوم فى آن واحد بينما تتناسب طرديا مع زيادة أحد العنصرين.

**Keywords:** Weldability of 7*xxx* series aluminum alloy, Heat treatable aluminum alloy, 7*xxx* series aluminum alloy, Al-Zn-Mg-Cu alloy, Mg effect, Cu effect

## 1. Introduction

The heat-treatable aluminum alloys provide good strength and toughness in engineering applications while maintaining the low density and high corrosion resistance of aluminum. These attributes allow the heat-treatable alloys to be used in a wide variety of applications [1-10], which include the aerospace, aircraft construction, transportation, truck trailers, railcars, armor plate, shipbuilding, tankage, piping, and appliance industries. The majority of these alloys are easily welded by the conventional arc welding processes (GMAW and GTAW), resistance spot and seam welding processes, as well as the high-energy processes (laser-beam and electron-beam welding), but there are a fair number of them that are not, including 7xxx series alloys which exhibit a wide range of crack sensitivity during welding. In addition, the weldable 7xxx series alloys produce greater sensitivity to corrosion after welding [11-16].

### *1.1. Weld cracking*

Weld cracking in aluminum alloys may be classified into two primary categories based on

the mechanism responsible for cracking and the crack location; solidification cracking and liquation cracking. Solidification cracking takes place within the weld fusion zone and typically appears along the center of the weld or at termination craters. Liquation cracks occur adjacent to the fusion zone and may or may not be readily apparent.

*1.2. Solidification cracking or hot tearing*

Solidification cracking or hot tearing occurs when high levels of thermal stress and solidification shrinkage are present while the weld pool is undergoing various degrees of solidification. The hot tearing sensitivity of any given aluminum alloy is influenced by a combination of mechanical, thermal, and metallurgical factors [17-20]. High heat inputs, such as high currents and slow welding speeds, are believed to contribute to weld solidification cracking [21].

*1.3. Liquation cracking*

An important element of the HAZ for precipitation-hardenable alloys is the thin boundary layer adjacent to the fusion zone that is referred to as the partially melted region. This region is produced when eutectic phases or constituents that have low melting points (melting points below the melting points of the bulk material) liquate, or melt, at grain boundaries during welding [22-24]. It occurs in precipitation-hardenable alloys because of the relatively large amount of alloying additions available to form eutectic phases. During welding, these phases liquate and, if sufficient stress is present, may be accompanied by tears. Under extreme conditions, continuous crack may form along the fusion zone interface.

*1.4. Porosity during welding*

The high solubility of hydrogen in molten aluminum can result in gas porosity when hydrogen gas is entrapped during solidification [25-29] unless proper precautions are heeded. Hydrogen has an appreciable solubility in molten aluminum and a low solubility in the solid. Hydrogen is absorbed into the molten pool during welding because of its high solubility, and it forms gas pores upon solidification due to the decrease in solubility. It is this difference in solubility that is the driving force for porosity formation [30]. The sources of hydrogen present in the welding system depend on the particular welding process. In arc welding these sources are hydrogen from the base metal, hydrogen from the filler metal, and hydrogen within the shielding gas [31]. During GTAW, ac with sufficient electrode-positive polarity provides excellent arc cleaning action to remove surface oxides.

*1.5. Alloying additions*

High strength in the 7xxx alloys is achieved by alloying additions of zinc, magnesium, and often copper, combined with controlled thermal and mechanical processing. Copper, in combination with zinc and magnesium in the 7xxx series alloys, increases strength but hampers weldability due to increased susceptibility to weld cracking. Alloy 7075, containing nominally 5.6% Zn, 2.5% Mg, and 1.6% Cu, is a commonly used alloy of this system, but it has a propensity for weld cracking.

*1.6. Dissimilar welding*

The introduction of aluminum alloys into wide variety of applications-as mentioned above-such as aerospace, aircraft and automobile productions has spurred intention in new alloys and the fabrication issues associated with these alloys. For example, various parts in automobile such as inner body panels, heat shields, structural parts, and body components are made from different aluminum alloys and series. Accordingly, dissimilar welds will be required between different aluminum alloys in a number of applications. The information in the literature that addresses the issues of dissimilar aluminum joining or provides guidelines on weldability is little [11, 32-36].

*1.7. This research*

This research discusses the various effects of alloying elements specially Cu and Mg con-

tents on welding of Al-Zn-Mg-Cu alloy (7*xxx* series) in both conditions of similar and dissimilar joining. Five series having different chemical compositions have been adopted to investigate welding of such alloys. Both similar and dissimilar welded joints have been made through various combinations of such alloys. Examination of mechanical properties of the welded joints; tensile strength and hardness values, were carried out coupled with microstructure examination for the alloys before and after welding. This research could explain the effects of alloying additions; Cu and Mg, on welding of such Al-Zn-Mg-Cu-based alloys.

## 2. Experimental work

### *2.1. Casting*

Al-Zn-Mg-Cu- based 7xxx-series alloy has been produced using resistance-furnace for melting and then cast in a metallic mould. Different compositions for such alloy were produced based mainly on changing the weight percentage of Mg and Cu in the range of 0 to 3 % each, producing 5 series of Al-Zn-Mg-Cu alloy. Table 1 shows the chemical composition of these five alloys. The as cast aluminum alloys were first homogenized at 400°C for about 4 hours followed by furnace cooling in a Muffle furnace.

### *2.2. Welding*

#### *2.2.1. Similar welding*

The five different compositions of Al-Zn-Mg-Cu alloys have been welded using TIG (GTAW) welding process forming five joints of similar combinations: 1-1, 2-2, 3-3, 4-4 and 5-5. Joint design has been chosen according to AWS recommendation for aluminum components. Typical representation for joint design is shown in fig. 1-a. Welding passes have been laid down in the sequence shown in fig. 2-a. Welding conditions for all welded joints are summarized in table 2. Filler wire was adopted for such type of aluminum alloy, to be AWS 5356 with chemical composition listed in table 3.

Joints 1-1, 2-2, 3-3 and 5-5 were successfully welded with four passes each as shown in fig. 3, but joint 4-4 showed dramatic behavior where complete separation had occurred in the welded joint at weld center line after performing the second pass as a result of solidification cracking as shown in fig. 4.

#### *2.2.2. Dissimilar welding*

Dissimilar joints were performed using the alloy series having the chemical composition shown in table 1. Joints have been designed in order to study various effects of the main alloying elements characterizing this aluminum alloy which are Mg and/or Cu. Zinc was not considered as it was kept nearly constant through all the five specimens. Joint combinations are listed in table 4 which shows the welding conditions for each joint.

Joint design has slightly been changed through increasing the included angle of the V-groove to be 90° instead of 60° as shown in fig. 1-b. This is because the dissimilar joint needs more caution in joining different metals, wider groove helps in keeping the different two metals away from melting together and keeps the joining occurs through filler wire combination with each side of the joint. As a result, the number of passes has increased from 4 to 6 passes as clearly shown in fig. 2-b. Filler wire was chosen to be similar to that one employed in similar welding, namely AWS 5356. The seven joints were successfully welded.

### *2.3. Mechanical testing of cast material and welded joints*

#### *2.3.1. Tension test*

Specimen with configuration shown in fig. 5 [37] was employed in tension test using Shimadzu-type testing machine with 10 Ton capacity. Tensile test specimens for base metal in as cast state, similar and dissimilar welded joints were designed according to AWS standard as depicted in fig. 5. These specimens were machined by milling and shaping. Joint 3-3 was damaged during machining because of its great brittleness. Therefore, tensile testing was performed to joints 1-1, 2-2 and 5-5 only.

Table 1
Chemical composition of cast materials

| Specimen No | Si | Fe | Cu | Mn | Mg | Cr | Ni | Zn | V | Pb | Ti | Al |
|---|---|---|---|---|---|---|---|---|---|---|---|---|
| 1 | 0.0433 | 0.127 | 2.83 | 0.00036 | 0.00631 | 0.00010 | 0.00040 | 6.47 | 0.00087 | 0.00294 | 0.00013 | rem |
| 2 | 0.0389 | 0.114 | 2.43 | 0.00228 | 1.27 | 0.00010 | 0.00040 | 5.4 | 0.00237 | 0.00238 | 0.00010 | rem |
| 3 | 0.0383 | 0.107 | 2.42 | 0.00370 | 2.35 | 0.00010 | 0.00040 | 5.68 | 0.00375 | 0.00175 | 0.00016 | rem |
| 4 | 0.0323 | 0.0932 | 1.17 | 0.00371 | 2.36 | 0.00010 | 0.00040 | 5.34 | 0.00379 | 0.00078 | 0.00010 | rem |
| 5 | 0.0254 | 0.100 | 0.0419 | 0.00355 | 2.40 | 0.00010 | 0.00040 | 5.48 | 0.00361 | 0.00060 | 0.00082 | rem |

Table 2
Welding conditions for similar joints

| Joint 1-1 | | | | | |
|---|---|---|---|---|---|
| | A | V | T | S | H.I. |
| Pass 1 | 140 | 13.4 | 80 | 0.6 | 3127 |
| Pass 2 | 140 | 13.4 | 18 | 2.667 | 703.5 |
| Pass 3 | 114 | 14.1 | 23 | 2.087 | 770.2 |
| Pass 4 | 114 | 14.1 | 25 | 1.92 | 837.2 |
| Total | 4 Passes | | | | 5438 |

| Joint 2-2 | | | | | |
|---|---|---|---|---|---|
| | A | V | T | S | H.I. |
| | 140 | 16 | 36 | 1.333 | 1680 |
| | 140 | 16 | 16 | 3 | 746.7 |
| | 110 | 15 | 20 | 2.4 | 687.5 |
| | 110 | 15 | 24 | 2 | 825 |
| | 4 Passes | | | | 3939 |

| Joint 3-3 | | | | | |
|---|---|---|---|---|---|
| | A | V | T | S | H.I. |
| | 121 | 15 | 50 | 0.96 | 1891 |
| | 121 | 15 | 33 | 1.455 | 1248 |
| | 110 | 15 | 25 | 1.92 | 859.4 |
| | 110 | 15 | 40 | 1.2 | 1375 |
| | 4 Passes | | | | 5373 |

| Joint 4-4 | | | | | |
|---|---|---|---|---|---|
| | A | V | T | S | H.I. |
| Pass 1 | 111 | 16 | 60 | 0.8 | 2220 |
| Pass 2 | 111 | 16 | 45 | 1.067 | 1665 |
| Pass 3 | --- | --- | --- | --- | --- |
| Pass 4 | --- | --- | --- | --- | --- |
| Total | 2 Passes - Failure : Center line crack | | | | 3885 |

| Joint 5-5 | | | | |
|---|---|---|---|---|
| A | V | T | S | H.I. |
| 111 | 16 | 63 | 0.762 | 2331 |
| 111 | 16 | 43 | 1.116 | 1591 |
| 105 | 18 | 33 | 1.455 | 1299 |
| 105 | 18 | 53 | 0.906 | 2087 |
| 4 Passes | | | | 7308 |

| | |
|---|---|
| A | Amperage |
| V | Voltage |
| T | Time (sec) |
| S | Speed (mm/sec) |
| H.I. | Heat input Joule/mm |
| L | Weld length (48 mm) |

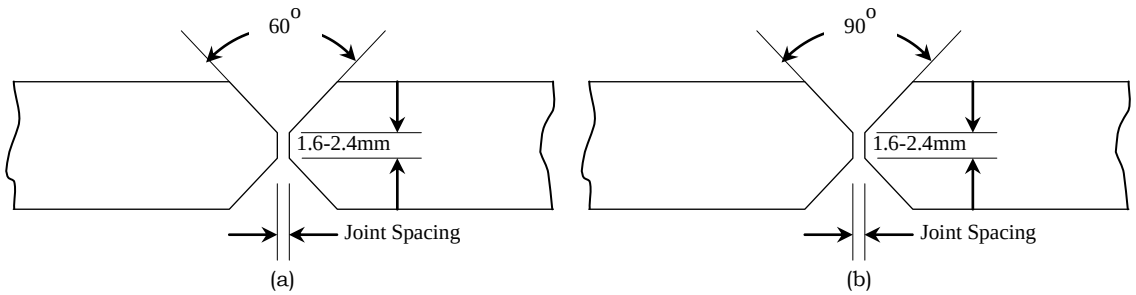

Fig. 1. Typical joint geometry used for GTAW of aluminum components. Source: American Welding Society.

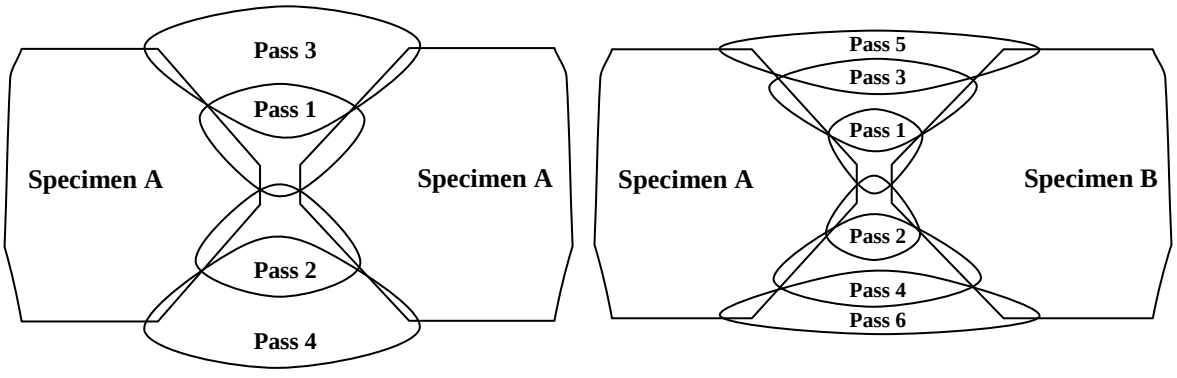

Fig. 2. Welding sequence followed in (a) similar welding and (b) dissimilar welding.

Table 3
Chemical composition for filler wire used with TIG process

| Element | Si | Cu | Mn | Mg | Cr | Ti | Al |
|---|---|---|---|---|---|---|---|
| 5356 | ... | ... | 0.12 | 5.0 | 0.12 | 0.13 | rem |

Table 4
Welding conditions for dissimilar joints

Joint 1-3

| | A | V | T | S | H.I. |
|---|---|---|---|---|---|
| Pass 1 | 173 | 12 | 43 | 1.233 | 1684 |
| Pass 2 | 148 | 13 | 19 | 2.789 | 689.7 |
| Pass 3 | 144 | 14 | 20 | 2.65 | 760.8 |
| Pass 4 | 94 | 13 | 69 | 0.768 | 1591 |
| Pass 5 | 94 | 12 | 33 | 1.606 | 702.3 |
| Pass 6 | 94 | 12 | 32 | 1.656 | 681.1 |
| Total | | 6 Passes | | | 6109 |

Joint 1-4

| | A | V | T | S | H.I. |
|---|---|---|---|---|---|
| Pass 1 | 148 | 11 | 41 | 1.293 | 1259 |
| Pass 2 | 148 | 11 | 25 | 2.12 | 767.9 |
| Pass 3 | 133 | 11.8 | 40 | 1.325 | 1184 |
| Pass 4 | 99 | 11.1 | 43 | 1.233 | 891.6 |
| Pass 5 | 59 | 11.5 | 87 | 0.609 | 1114 |
| Pass 6 | 59 | 11.2 | 58 | 0.914 | 723.1 |
| Total | | 6 Passes | | | 5940 |

Joint 2-3

| | A | V | T | S | H.I. |
|---|---|---|---|---|---|
| Pass 1 | 173 | 11.5 | 35 | 1.514 | 1314 |
| Pass 2 | 173 | 11.5 | 18 | 2.944 | 675.7 |
| Pass 3 | 119 | 11.2 | 25 | 2.12 | 628.7 |
| Pass 4 | 119 | 11.3 | 22 | 2.409 | 558.2 |
| Pass 5 | 92 | 11.1 | 45 | 1.178 | 867.1 |
| Pass 6 | 92 | 11.2 | 20 | 2.65 | 388.8 |
| Total | | 6 Passes | | | 4432 |

Joint 2-4

| | A | V | T | S | H.I. |
|---|---|---|---|---|---|
| Pass 1 | 160 | 11.1 | 40 | 1.325 | 1340 |
| Pass 2 | 186 | 12 | 17 | 3.118 | 715.9 |
| Pass 3 | 95 | 11 | 45 | 1.178 | 887.3 |
| Pass 4 | 95 | 11 | 40 | 1.325 | 788.7 |
| Pass 5 | 95 | 11 | 40 | 1.325 | 788.7 |
| Pass 6 | 79 | 11 | 38 | 1.395 | 623.1 |
| Total | | 6 Passes | | | 5144 |

Joint 3-4

| | A | V | T | S | H.I. |
|---|---|---|---|---|---|
| Pass 1 | 152 | 11 | 42 | 1.262 | 1325 |
| Pass 2 | 174 | 12.5 | 15 | 3.533 | 615.6 |
| Pass 3 | 136 | 11 | 29 | 1.828 | 818.6 |
| Pass 4 | 109 | 11 | 30 | 1.767 | 678.7 |
| Pass 5 | 91 | 10.8 | 35 | 1.514 | 649 |
| Pass 6 | 76 | 11 | 48 | 1.104 | 757.1 |
| Total | | 6 Passes | | | 4844 |

Joint 3-5

| | A | V | T | S | H.I. |
|---|---|---|---|---|---|
| Pass 1 | 165 | 11.6 | 42 | 1.262 | 1517 |
| Pass 2 | 189 | 11.5 | 18 | 2.944 | 738.2 |
| Pass 3 | 155 | 11 | 11 | 4.818 | 353.9 |
| Pass 4 | 107 | 11 | 35 | 1.514 | 777.3 |
| Pass 5 | 71 | 11 | 60 | 0.883 | 884.2 |
| Pass 6 | 71 | 11 | 35 | 1.514 | 515.8 |
| Total | | 6 Passes | | | 4786 |

Joint 4-5

| | A | V | T | S | H.I. |
|---|---|---|---|---|---|
| Pass 1 | 189 | 11 | 37 | 1.432 | 1451 |
| Pass 2 | 189 | 11 | 14 | 3.786 | 549.2 |
| Pass 3 | 167 | 11 | 22 | 2.409 | 762.5 |
| Pass 4 | 107 | 11 | 28 | 1.893 | 621.8 |
| Pass 5 | 71 | 10 | 52 | 1.019 | 696.6 |
| Pass 6 | 71 | 10 | 42 | 1.262 | 562.6 |
| Total | | 6 Passes | | | 4644 |

| | |
|---|---|
| A | Amperage |
| V | Voltage |
| T | Time (sec) |
| S | Speed (mm/sec) |
| H.I. | Heat input Joule/mm |
| L | Weld length (53 mm) |

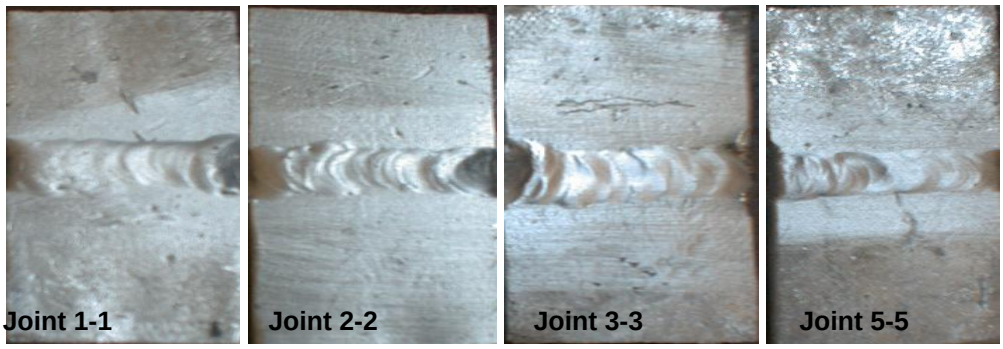


Fig. 3. Successfully similar welded joints.

Fig. 4. Failed specimen no. 4 which fractured after second pass.

*2.3.2. Microhardness test*

Microhardness was measured for all series adopted in this study for base metal and welded joints using Shimadzu microhardness tester. For welded specimens the microhardness was measured at various positions taking into consideration the base metal (BM), heat affected zone (HAZ), fusion zone (FZ), and weld metal (WM).

## 3. Results and discussion

*3.1. Microstructure of as cast alloys and welded joints*

*3.1.1. As cast alloys*

The microstructure has been investigated through optical Zeis-Model microscope. Microstructures for specimens before welding (as cast) are shown in fig. 6. It is obvious from the figure that dendritic structure is prevailing for all specimens. Fig. 6-a shows high precipitates at grain boundaries of specimen 1 while specimens 2, 3 and 4 show precipitates on grain boundaries and on areas almost near them as shown in fig. 6-a, b and c. Specimen 5 does not show any precipitates on grain boundaries but on the grain itself with higher density compared to other specimens.

*3.1.2. Welded joints*

For similar welded joints microstructures are shown for different combinations in figs. 7 through 11. For joint 1-1 depicted in fig. 7, the structure of pass 1 is much finer than pass 3, as the heating during pass 3 causes a grain coarsening.

Figure 8 compares the microstructures of both base metals before and after welding for joint 2-2. Structure of the base metal became coarser after welding. This probably occurred due to the relatively small size welded specimens. Increasing the precipitation density on grain boundaries and inside the grains can be easily noticed in fig. 9. In this figure precipitates inside WM became very dense over the grains, while it decreases along grain boundaries over WM region, in addition, precipitates at HAZ takes large shape. Generally, the size of precipitates decreases from HAZ towards WM.

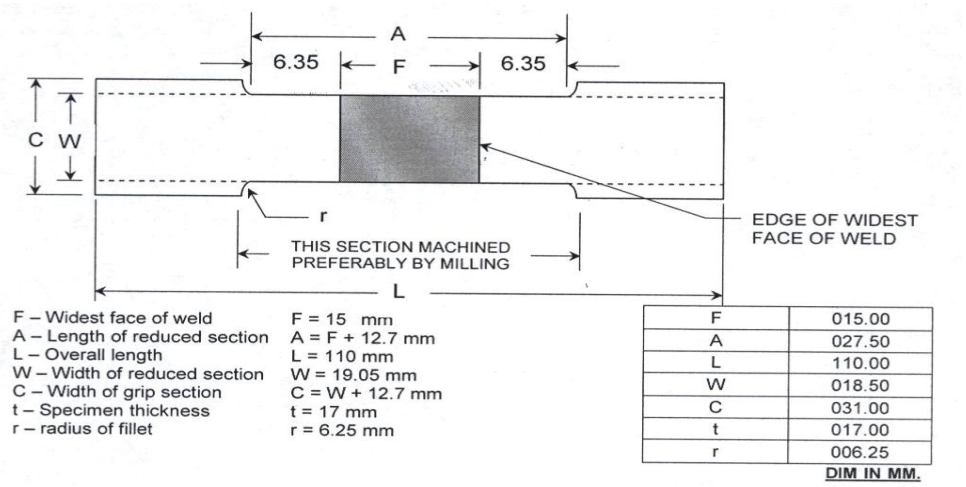


Fig. 5. Reduced-section tension specimen [37].

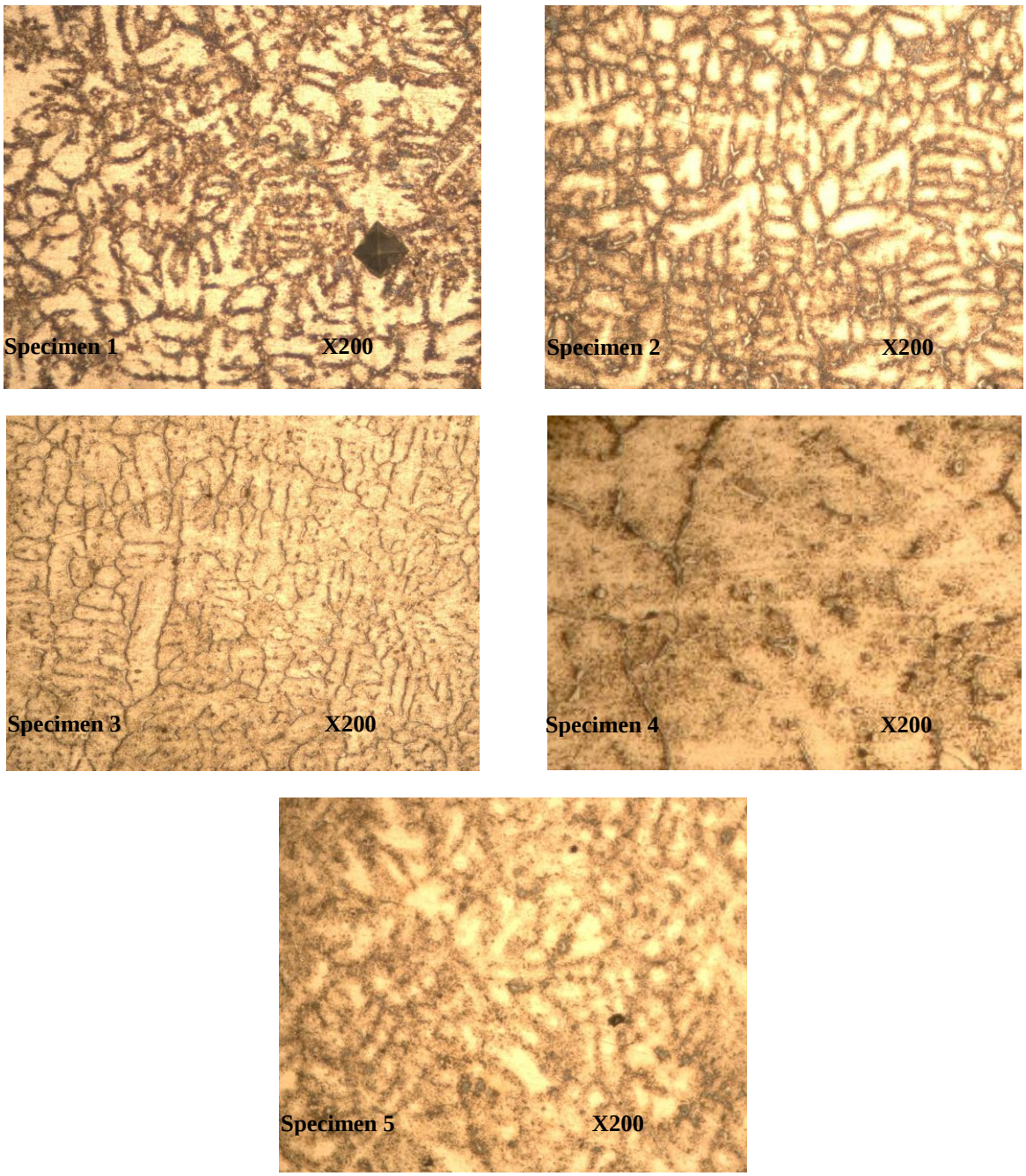


Fig. 6. Microstructure for as cast material.

Fig. 10 shows pass 2 for joint 2-2 which indicates the increase in precipitates beside grain boundaries due to heat treatment occurring as a result of subsequent passes. Fig. 11 shows the microstructure difference at the locations WM-pass 1, HAZ and BM of joint 3-3. Columnar-shape grains are representing the HAZ region while pass 1 keeps its equiaxed shape. Heat inputs of subsequent passes heat treated the first pass and its nearby areas of HAZ and BM. It is also noticed that the precipitates are denser at the HAZ region than the WM.

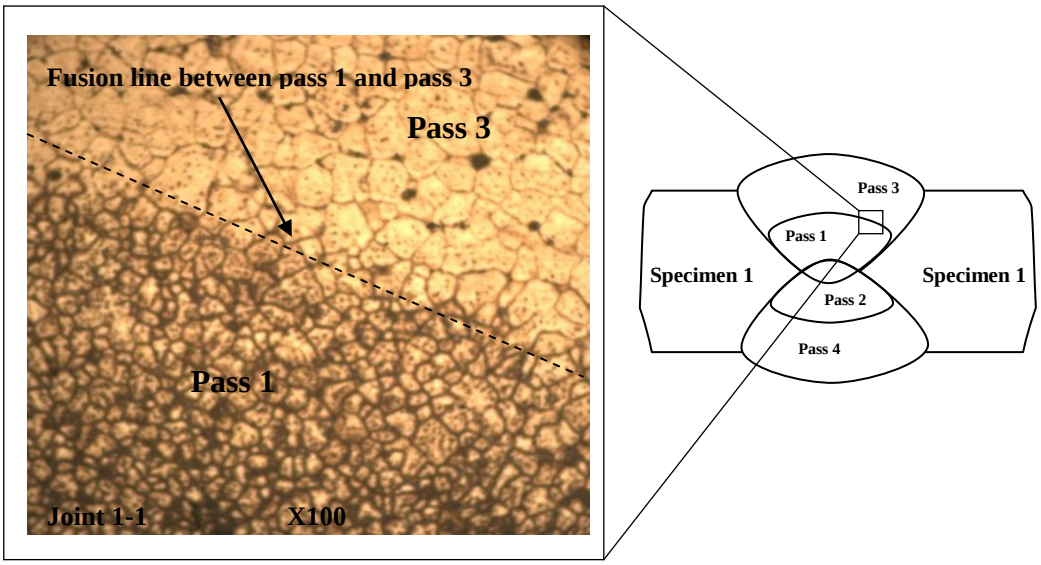


Fig. 7 Similar joint 1-1.

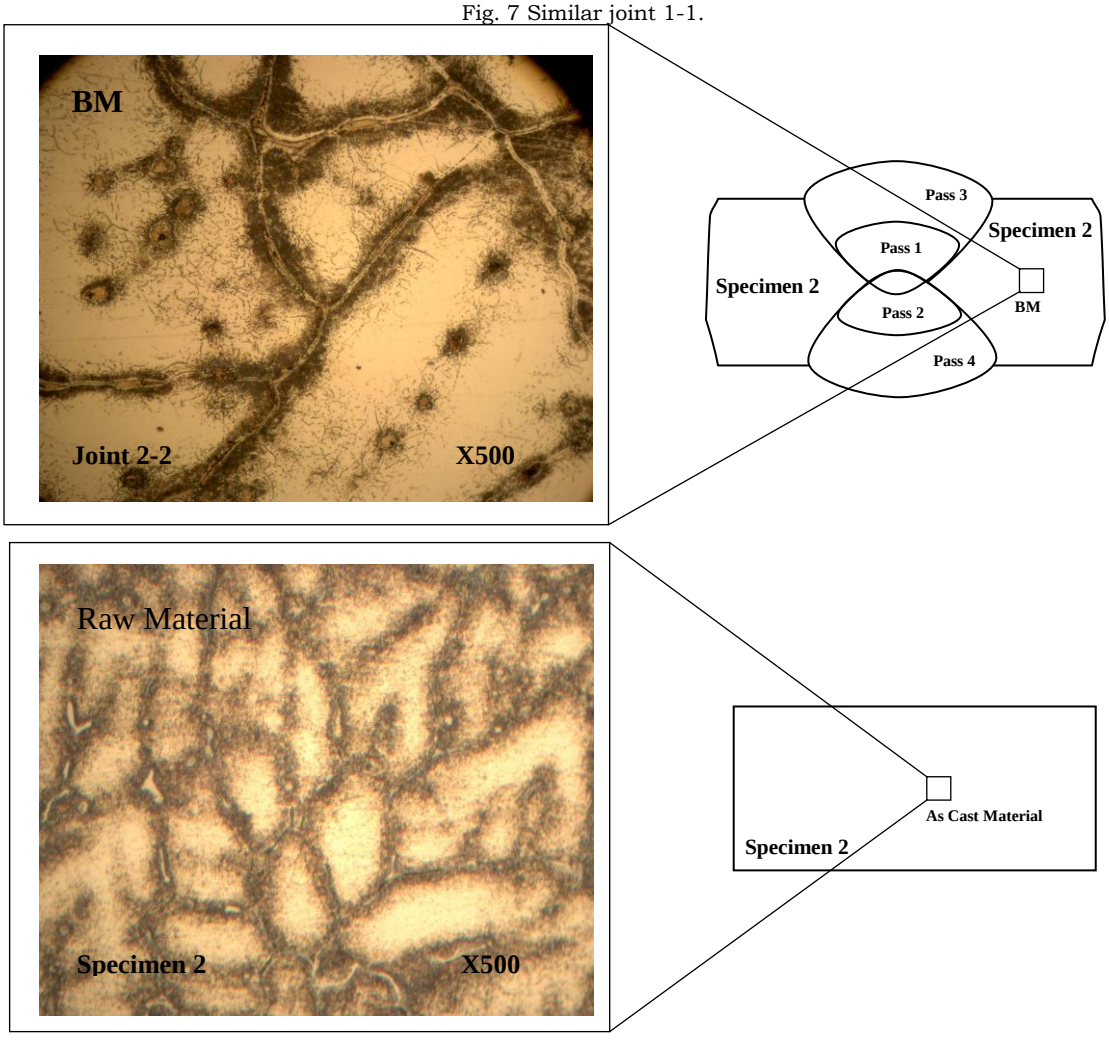


Fig. 8. Microstructure before and after welding of specimen 2.

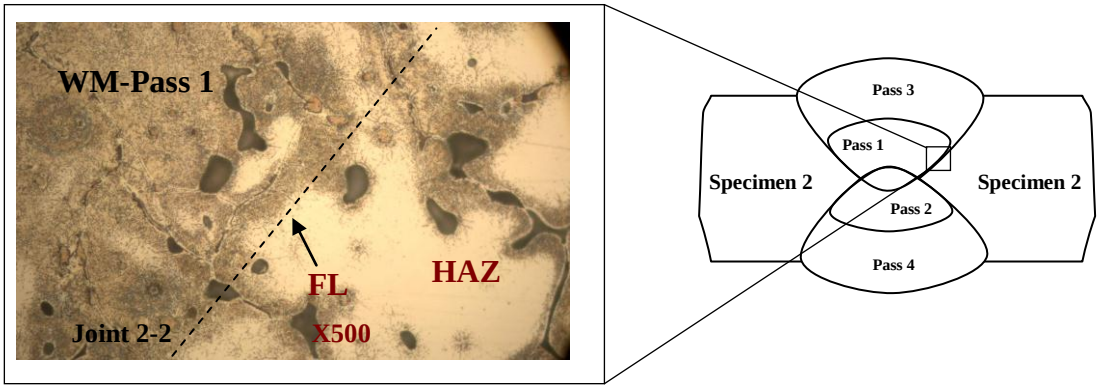


Fig. 9. Microstructure of similar joint 2-2.

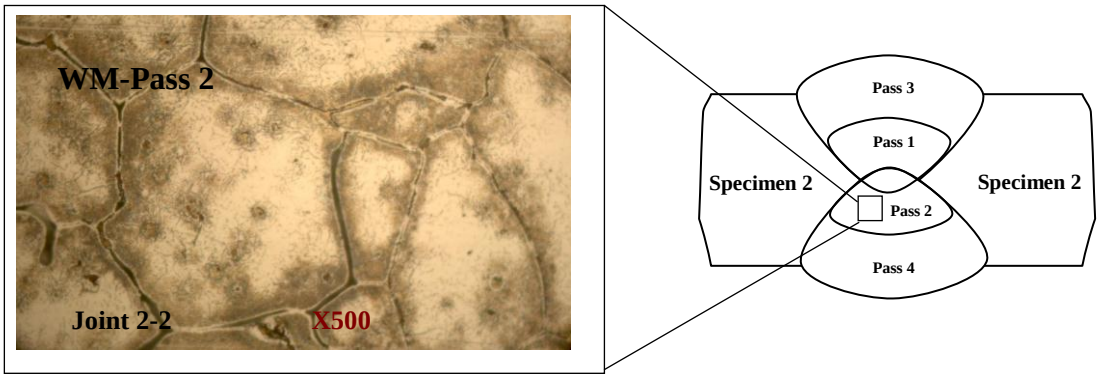


Fig. 10. Microstructure at different location of similar joint 2-2.

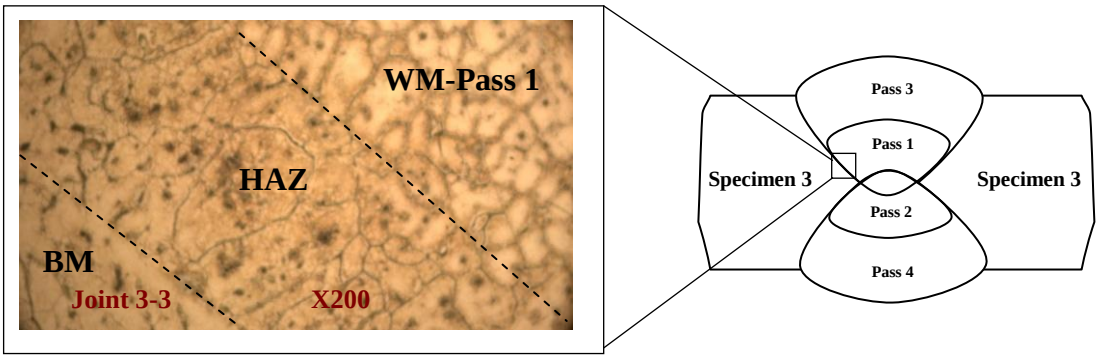


Fig. 11. Microstructure of similar joint 3-3.

*3.2. Fracture surface of dissimilar joints*

Fracture surface/appearance for selected samples from similar and dissimilar joints subjected to tension was examined. In dissimilar welded joints fracture occurred either in the side of material 3 or material 4 in all joints as shown in fig. 12 for example. In case of joints 1-4 and 2-4, fracture occurred at FZ between WM and Material 4. While fracture occurred in FZ between WM and Material 3 in joint 1-3 and in BM of material 3 in joint 2-3.

Meanwhile, the fracture appearance is brittle in both materials 3 and 4 with different morphologies as shown in fig. 13. It is clear from the figure that columnar structure is dominant at outside surfaces of the specimens while the core is mainly equiaxed structure.

Depth of the columnar structure in observed fracture surface of specimen 4 is deeper than that in case of specimen 3. In addition, the equiaxed structure of specimen 4 showed coarser grains than that for specimen 3.

### 3.3. Mechanical properties for as cast material and welded joints

#### 3.3.1. Microhardness test results

For as cast material, the microhardness measurements were done at mainly two different locations; namely the areas with high precipitates and areas with low precipitates. Averages of readings of such specimens are summarized in table 5.

As shown in figs. 6-11, precipitates are distributed in very different manner for different chemical composition range of the 5 specimens. The results related to the first cast were of a special importance because of the dramatic behavior of some specimens either during welding or machining. For welded joints, results for microhardness measurements are schematically shown in fig. 14.

#### 3.3.2. Stress-strain relations

Fig. 15 demonstrates the stress-strain diagrams for as cast materials, similar and dissimilar joints. From the figure, it is clear that the as cast materials exhibit the higher values of tensile strength and strain in general compared with welded joints. In the same time, specimens 3 and 4 recorded the lower tensile strength values with very low ductility, while specimens 5 and 1 recorded the higher tensile strength values with much better ductility.


Fig. 12 Example for fractured specimens after tensile testing.

3-1 4-2

Fig. 13. Fractography for tensile-tested dissimilar-welded joints 3-1 and 4-2.

Table 5
Microhardness measurements for raw material

| Specimen | 1 | | 2 | | 3 | | 4 | | 5 | |
|---|---|---|---|---|---|---|---|---|---|---|
| Precipitates | L.P. | H.P. | L.P. | H.P. | L.P. | H.P. | L.P. | H.P. | L.P. | H.P. |
| Microhardness, Hv. | 55 | 45 | 68 | 55 | 75 | 61 | 67 | 54 | 70 | 60 |

Load 100 gm for 10 sec. L.P: Low precipitates, H.P. High precipitates.

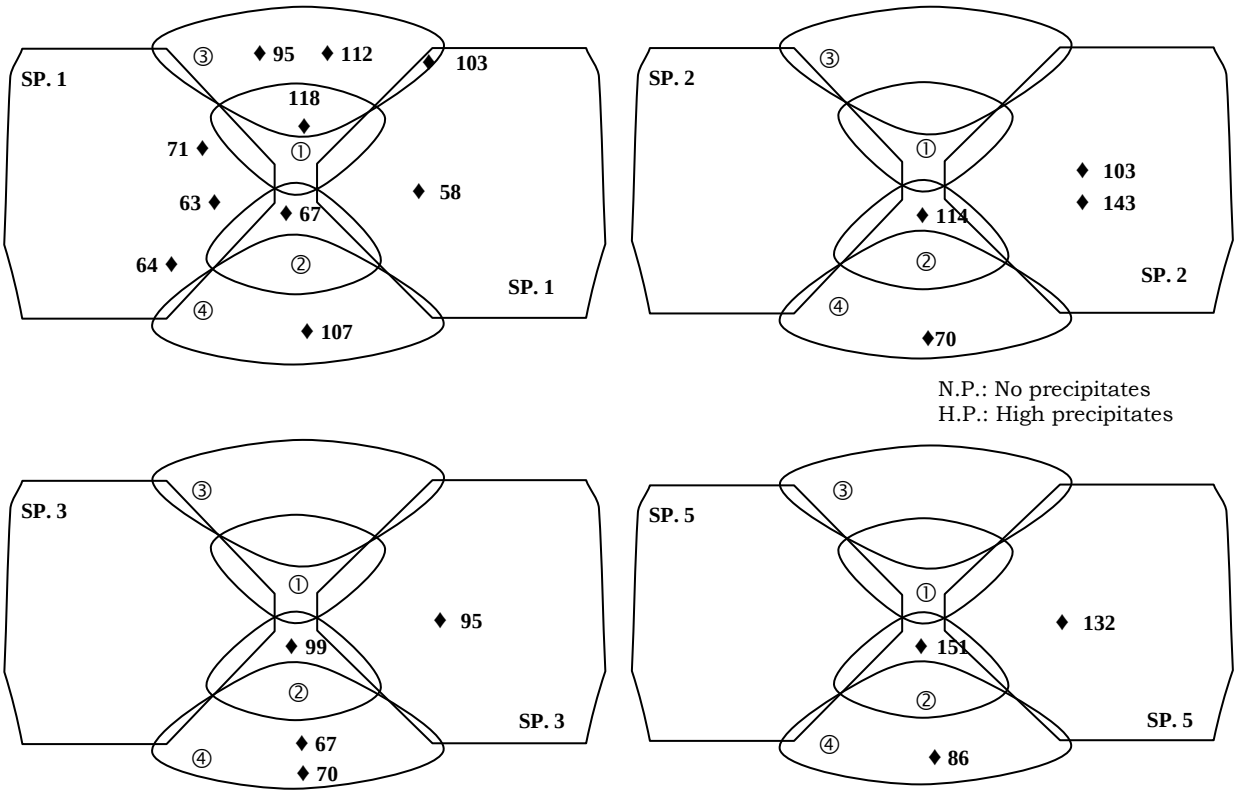


Fig. 14. Microhardness for similar welded joints (load 200 gm).

Concerning similar welded joints, it is worth mentioning that welding had dramatically deteriorated the mechanical properties of all specimens from 1 to 5. In comparison between the tensile strength values for raw materials and similar joints of the same material, it is clear that there is an inverse relationship. For example, specimen 5 showed only 50% of its tensile strength value before welding and in the other hand, specimen 2 lost about 76% of its original tensile value before welding as depicted in details in table 6.

Stress and strain values for dissimilar welded joints are in a good agreement with the previously concluded remarks for the raw material and similar welded joints. This can be explained by the great decrease in tensile strength and strain values of all joints having either specimen 3 or 4. As shown in table 6, these specimens showed the lowest tensile strength values before welding. Therefore, it is expected that specimens 3 and 4 will show only 10 to 15% of its original tensile strength values before welding. From fig. 16 the value of tensile strength recorded for joint 3-4 was obviously the minimum.

Table 6
Reduction % in tensile strength due to similar welding

| Raw and similar joint | $\sigma_t$ Raw material, MPa | $\sigma_t$ , Similar joint, MPa | Reduction % in tensile strength |
|---|---|---|---|
| 1 and 1-1 | 203 | 62 | 69.45812 |
| 2 and 2-2 | 163 | 40 | 75.46012 |
| 3 and 3-3 | 102 | ... | ... |
| 4 and 4-4 | 153 | ... | ... |
| 5 and 5-5 | 221 | 111 | 49.77375 |

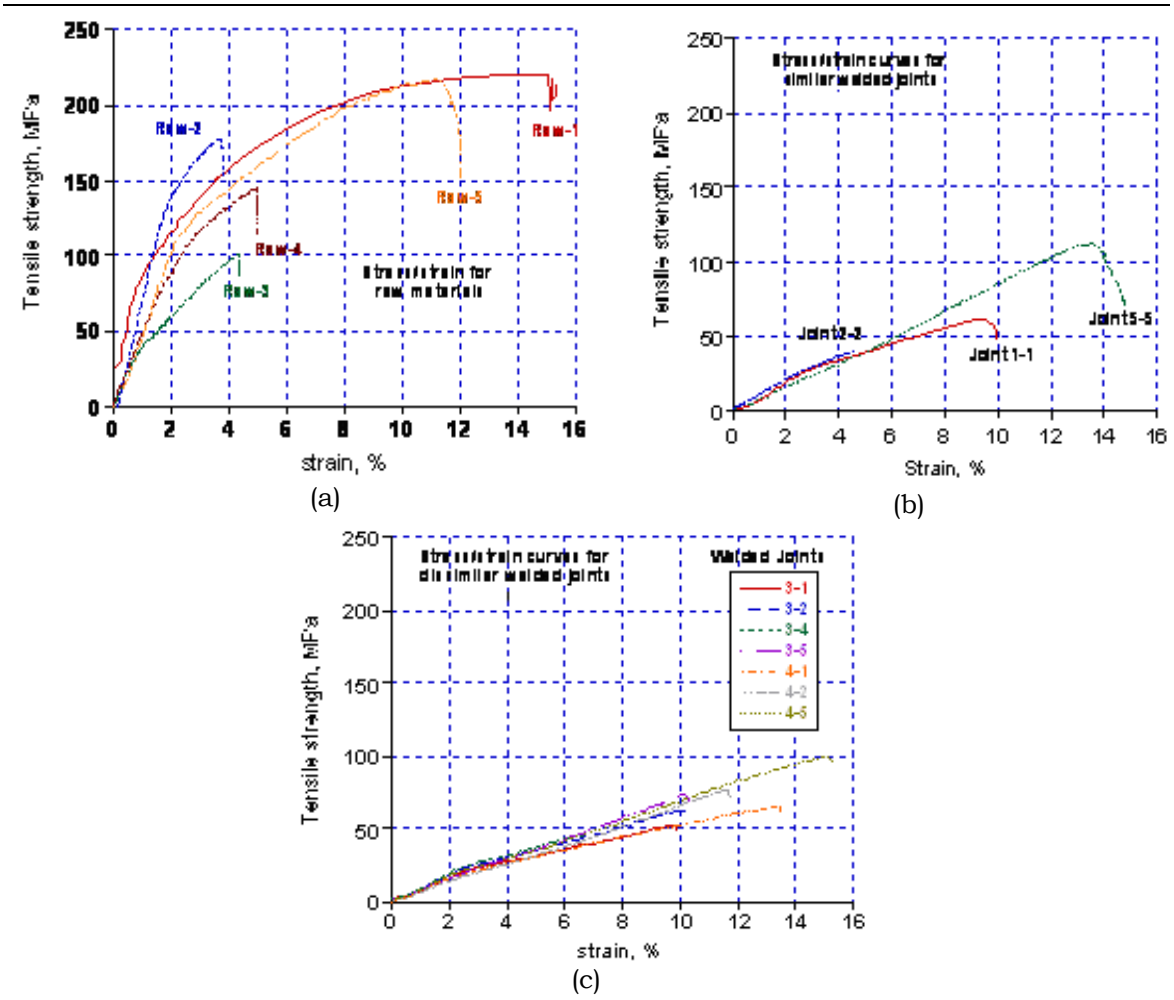


Fig. 15. Stress strain curves for raw materials, similar and dissimilar joints.

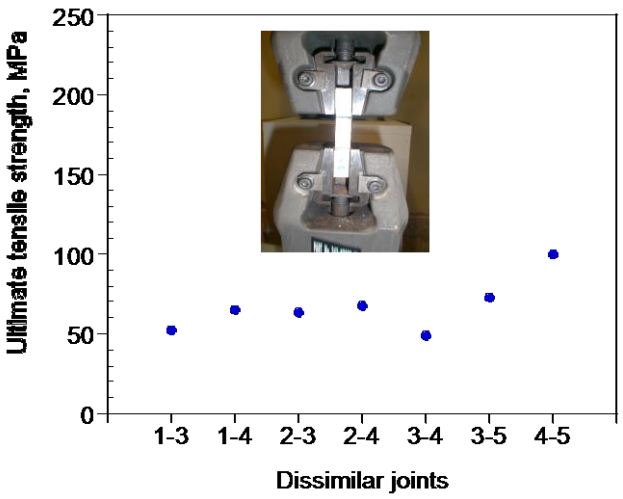


| Dissimilar Joint | Ultimate tensile strength, MPa | Place of Fracture |
|---|---|---|
| 1-3 | 53 | FZ3 |
| 1-4 | 65 | FZ4 |
| 2-3 | 64 | BM3 |
| 2-4 | 68 | FZ4 |
| 3-4 | 49 | BM3 |
| 3-5 | 73 | BM3 |
| 4-5 | 100 | BM4 |

Fig. 16. Ultimate tensile strength recorded for dissimilar joints.

Fig. 17 summarizes the relationship between ultimate tensile strength of as cast material and all welded joints. Chemical composition of the used material has been added to the figure for studying the effect of alloying elements on mechanical behavior of the material.

Specimen 5 with almost 0%Cu, 2.4% Mg, and 5.48% Zn, showed maximum tensile strength, on the other hand specimen 1 with 2.83% Cu, almost 0% Mg, and 6.47% Zn revealed the second highest value among other specimens. Combination of higher values for Cu and Mg to reach 3% each in specimen 3 leads to remarkable decrease in tensile strength of the specimen. This is attributed to both existences of Cu and Mg with high percentage which leads to high sensitivity to cracking when arc welded which generally discourages the use of arc welding application of Al-Zn-Mg-Cu alloy 7xxx. Decreasing Cu content and/or Mg content is expected to improve the welding results of such alloy. Because Zn content was kept constant in all five tested specimens, its effect on mechanical properties can be neglected. Welding highly decreased the tensile strength of all specimens as shown in fig. 17.

## 4. Conclusions

This research investigated the effect of Cu and Mg contents on the weldability of Al-Zn-Mg-Cu- based 7*xxx* series alloy in both cases of similar and dissimilar welding. The research could draw the following concluding remarks:

- Welding highly decreased the mechanical properties, namely tensile strength, of the investigated material either in case of similar or dissimilar welded joints.
- Increasing Cu content to about 2.83 wt% with almost zero Mg showed the best tensile strength either in similar or dissimilar welded joints. Same results could be obtained with maximum content of Mg 2.4 wt% and almost zero Cu.
- Increasing both Cu and Mg contents to 2.42 wt% and 2.53 wt%, respectively in the same time deteriorated the tensile strength for similar and dissimilar welded joints.
- Properties obtained after welding of Al-Zn-Mg-Cu alloy has an inverse relation with combined increase of Cu and Mg content while it has a direct relation with single increase of either Cu or Mg alloying addition.

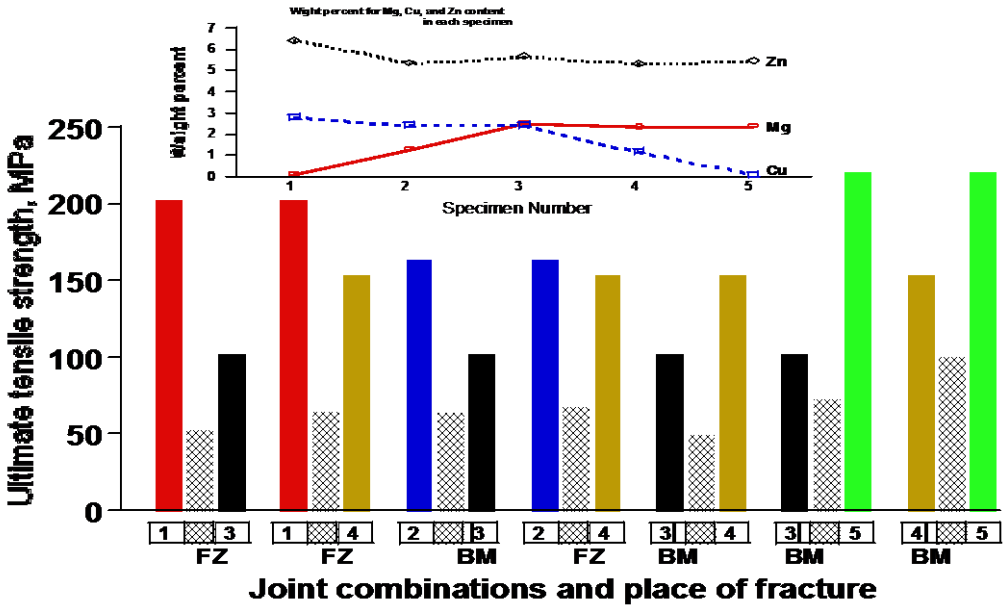


Fig. 17. Tensile strength for dissimilar welded joints with different chemical compositions compared with original tensile strength of base materials.

- The microstructure of all cast series of 7*xxx* alloys showed dendritic structure but with different distribution for precipitates. High precipitates at the grain boundaries of specimen with maximum Cu content -in this study-; 2.83 wt% and minimum Mg content about 0 wt%. Alloy with Minimum Cu content; about 0 wt% and maximum Mg content –in this study-; 2.4 wt% does not show any precipitates at the grain boundaries but inside the grain itself with higher density than other alloys. Alloys with moderate Cu and Mg contents ranging from 1.27 to 2.36 wt% for Mg and from 1.17 to 2.43 wt% for Cu showed precipitates at the grain boundaries and at areas almost near them.

**References**


[1] A. Witry, M.H. Al-Hajeri and Ali A. Bondok, "Thermal Performance of Automotive Aluminum Plate Radiator", Applied Thermal Engineering, Vol. 25 (8-9), pp. 1207-1218 (2005).

[2] W. Speer and O. S. Es-Said, "Applications of an Aluminum-Beryllium Composite for Structural Aerospace Components", Engineering Failure Analysis, Vol. 11 (6), pp. 895-902 (2004).

[3] A. Kelkar, R. Roth and J. Clark, "Automobile Bodies: Can Aluminum Be an Economical Alternative to Steel?", Journal JOM, Vol. 53 (8), pp. 28-32 (2001).

[4] M. Nakai and T. Eto, "New Aspect of Development of High Strength Aluminum Alloys for Aerospace Applications", Material Science and Engineering A, Vol. 285 (1-2), pp. 62-68 (2000).

[5] A. Heinz, A. Haszler, C. Keidel, S. Moldenhauer, R. Benedictus and W. S. Miller, " Recent development in Aluminum Alloys for Aerospace Applications", ", Material Science and Engineering A, Vol. 280 (1), pp. 102-107 (2000).

[6] W.J. Poole, J.A. Saeter, J. Haung, G. Waterloo and S. Skjervold, "Microstructural Strengthening in Al-Zn-Mg-Cu Alloys Used in Automotive Bumpers", Automotive Alloys, Edited by S.K. Das, The Minerals, Metals & Materials Society (1999).

[7] F.H. Froes, "Advanced metals for aerospace and Automotive Use", ", Material Science and Engineering A, Vol. 184 (2), pp. 119-133 (1994).

[8] W.H. Hunt, "Cost Effective High Performance Aluminum Matrix Composited for Aerospace Applications", Metal Powder Report, Vol. 47, (2), p. 63 (1992).

[9] P. Gilman, "Rapidly Solidified Aluminum Alloys for Aerospace", International Journal of Fatigue, Vol. 13, (2), p. 185 (1991).

[10] R.C. Dorward and T.R. Pritchett, "Advanced Aluminum Alloys for Aircraft and Aerospace Applications", Vol. 9 (2), pp. 63-69 (1988).

[11] P.B. Srinivasa, W. Dietzel, R. Zettler, J.F. Dos Satos and V. Sivan, "Stress Corrosion Cracking Susceptibility of Friction Stir Welded AA7075-AA6056 Dissimilar Joint", Material Science and Engineering A, Vol. 392 (1-2), pp. 292-300 (2005).

[12] X.Y. Li, Y.G. Yan, L. Ma, Z.M. Xu and J.G. Li, "Cavitation Erosion and Corrosion Behavior of Copper-Manganese-Aluminum Alloy Weldment", Material Science and Engineering A, Vol. 382 (1-2), pp. 82-89 (2004).

[13] A.K. Jha, S.V.S.N. Murty, V. Diwakar and K.S. Kumar, "Metallurgical Analysis of Cracking in Weldment of Propellant Tank", Engineering Failure Analysis, Vol. 10 (3), pp. 265-273 (2003).

[14] P.S. Pao, S.J. Gill, C.R. Feng and K.K. Sankaran, "Corrosion-Fatigue Crack Growth in Friction Stir Welded Al 7050", Vol. 45 (5), pp. 605-612 (2001).

[15] R.P. Meister and D.C. Martin, "Welding of Aluminum and Aluminum Alloys", DMIC Report 236, Defense Metals Information Center, p. 65 (1967).

[16] K. Videm, "Corrosion of Aluminium Alloys in High Temperature Water – A Survey", Vol. 1 (2), pp. 145-153 (1959).

[17] E. Cicala, G. Duffet, H. Andrzejewski, D. Grevey and S. Ignat, "Hot Cracking in Al-Mg-Si Alloy Laser Welding – Operating Parameters and Their Effects", Material Science and Engineering A, In Press, Corrected Proof, Available Online, Feb. (2005).

[18] W. Liu, "Computational Analysis and Prediction of Weld-Solidification Cracking", Computational Materials Science, Vol. 4 (3), pp. 211-219 (1995).
[19] G.L. Makar, J. Kruger and K. Sieradzki, "Stress Corrosion of Rapidly Solidified Magnesium-Aluminum Alloys", Corrosion Science, Vol. 34 (8), pp. 1311-1323 (1993).
[20] C.E. Cross, W.T. Tack, L.W. Loechel, and L.S. Kramer, aluminum Weldability and Hot Tearing theory, Weldability of Materials, ASM International, pp 275-282 (1990).
[21] R.A. Chihoski, The Character of Stress Fields around a Weld Arc Moving on Aluminum Sheet, Welding J., Vol. 51 (1), p. 9-s (1972).
[22] Z.J. Lu, J.D. Parker, W.J. Evans and S. Birley, "Simulation of Microstructure and Liquation Cracking in 7017 Aluminum Alloy ", Material Science and Engineering A, Vol. 220 (1-2), pp. 1-7 (1996).
[23] R. Hermann, S.S. Birley and P. Holdway, "Liquation Cracking in Aluminum Alloy Welds", Material Science and Engineering A, Vol. 212 (2), pp. 247-255 (1996).
[24] S. Kou, Welding Metallurgy, John Wiley & Sons, p. 239 (1987).
[25] H. Fujii, H. Umakoshi, Y. Aoki and K. Nogi, "Bubble Formation in Aluminum Alloy During Electron Beam Welding", Journal of Materials Processing Technology, Vol. 155-156, pp. 1252-1255 (2004).
[26] A. Haboudou, P. Peyre, A.B. Vannes and G. Peix, "Reduction of Porosity Content Generated During Nd: YAG Laser Welding of A356 and AA5083 Aluminum Alloys", Material Science and Engineering A, Vol. 363 (1-2), pp. 40-52 (2003).
[27] J.L. Canaby, F. Blazy, J.F. Fries and J.P. Traverse, "Effects of High Temperature Surface Reactions of Aluminum-Lithium Alloy on Porosity of welded areas", Material Science and Engineering A, Vol. 136, pp. 131-139 (1991).
[28] D.G. Howden and D.R. Milner, Brit. Weld. J., Vol. 10, p. 304 (1963).
[29] Z.P. Saperstein, G.R. Prescott, and E.W. Monroe, Porosity in Aluminum Welds, Weld. J., Vol. 43 (10), 1964, p. 443-s (1963).
[30] M. Ueda and S. Ohno, Trans. Natl. Res. Inst. Met. (Jpn), Vol. 16, p. 2 (1974).
[31] R.P. Martukanitz and P.R. Michnuk, Sources of Porosity in Gas Metal Arc Welding of Aluminum, Aluminum, Vol. 58 (5), p. 276 (1982).
[32] A.C. Somasekharan and L.E. Murr, "Microstructures in Friction-Stir Welded Dissimilar magnesium Alloys and magnesium Alloys to 6061-T6 Aluminum Alloy", Materials Characterization, Vol. 52, pp. 49-64 (2004).
[33] J.M. Gomez de Salazar and M.I. Barrena, "Dissimilar Fusion Welding of AA7020/MMC Reinforced with $Al_2O_3$ Particles. Microstructure and Mechanical Properties", Material Science and Engineering A, Vol. 352, pp. 162-168 (2003).
[34] M.M. Mossman and J.C. Lippold, "Weldability Testing of Dissimilar Combinations of 5000- and 6000Series Aluminum Alloy", Welding Journal, Sept., pp. 188-s-194-s (2002).
[35] T. Luijendijk, "Welding of Dissimilar Aluminum Alloys", Journal of Materials Processing Technology, Vol. 103, pp. 29-35 (2000).
[36] C. Menzmer, P.C. Lam, T.S. Srivatsan and C.F. Wittel, "An Investigation of Fusion Zone Microstructures of Welded Aluminum Alloy Joints", Materials Letters, Vol. 41, pp. 192-197 (1999).
[37] American National Standard, Structural Welding Code, ANSI/AWS D1.1 (1998).

Received April 10, 2005
Accepted September 13, 2005